

Provided for non-commercial research and educational use only.  
Not for reproduction or distribution or commercial use.

		Volume 71, Number 4 February 15, 2007		
<b>Geochimica et Cosmochimica Acta</b>		JOURNAL OF THE GEOCHEMICAL SOCIETY AND THE METEORITICAL SOCIETY		
Executive Editor: FRANK A. PODOSEK	Editorial Manager: LINDA TOWER Editorial Assistants: KAREN POLLARD KATHY SIVILE	Webmaster: ROBERT H. NECKA, JR. Production Manager: CHRIS AUGER		
<b>ASSOCIATE EDITORS:</b> ROBERT C. ALLEN JERRY C. ALT YURI ARAKI CAROL ALBERTI MORTON BIRNBAUM LISA G. BONDIG JULIA A. BRADEN ALAN D. BRANDON DAVID J. BRIDGES ROBERT C. BURTON WILLIAM H. CAREY THOMAS CHAPMAN ANNE COOPER DAVID R. COLE LINDA J. COOPER	<b>EDITORIAL BOARD:</b> JOHN CHERRY ZHUOSHU DING CAROL M. EGGLETON JOSEF FALICKI JERRY B. FINE FREDERICK A. FINE ALAN B. GALBRAITH JANIS R. HARRIS T. MARK HARRISON H. ROSEMARY HAYRY GEORGE R. HALL GREGORY F. HAZEN JERRY HEWITT JIN-SHENG HONG KAREN JOHNSON CLARE JOHNSON	<b>EDITORIAL BOARD:</b> NORIKO KITA CHRISTIAN KUBIK RASHY KUMAR STEPHAN M. KRAMER S. KRIVONOSHI ALEXANDER N. KRUT JOSIE KUMAR GILGAIL A. LOGAN TIMOTHY J. LLOYD MERRILL L. MACHESKY BRANDON MANN JOSUÉ MORALES JAMES MURPHY MARTIN A. MURPHY JACK J. MURPHY DAVID W. NUTTALL	<b>EDITORIAL BOARD:</b> JOHN W. MURK ALFONSO MURCI BRIAN MURPHY HIDEO NAGAIWA MARTIN NIKOLIC PIETRI A. O'DAY ERIC H. OELGERS SANDRA PIZZARELLO BRIAN T. PIRI MARK ROSSIGNOL W. DAVI RYAN EDWARD M. RILEY CLAUDIA RISSOTTO J. KELLY RUSSELL SARA S. RUSSELL JOHN R. RYAN	<b>EDITORIAL BOARD:</b> F. J. RYBICKI JACQUES SCHOTT JAMES SHARPLEY TAMARA J. SLOW J. S. SODERBERG DASH OSCAR L. STANKE GABRIELE STROZZI DARREN A. SWENSON DAVID J. VAUGHAN ROBERT J. WALKER LARRY A. WALKER DAVID J. WILSON RUPERT WYLLIE ROY A. WOODRUFF CHUN ZHU
Volume 71, Number 4		February 15, 2007		
<b>Articles</b>				
J. S. COX, T. M. SEWARD: The hydrothermal reaction kinetics of aspartic acid .....	797			
S. D. KELLY, K. M. KIMMER, S. C. BROOKE: X-ray absorption spectroscopy identifies calcium-uranyl-carbonate complexes at environmental concentrations .....	821			
J. W. STUCKI, K. LEE, B. A. GOODMAN, J. E. KOSTRA: Effects of <i>in situ</i> biostimulation on iron mineral speciation in a sub-surface soil .....	835			
S. DE MOTTE, F. J. R. MEYERMAN, A. GUTAT, A. BOUDOU, S. SAUVAGE, M. GELINO: Cadmium transport in sediments by tubificid bioturbation: An assessment of model complexity .....	844			
A. GÉHIN, J.-M. GRENÉCHE, C. TOUKASSAT, J. BREMBÉ, D. G. RANCOOTY, L. CHARLET: Reversible surface-sorption-induced electron-transfer oxidation of Fe(II) at reactive sites on a synthetic clay mineral .....	863			
A. J. SLOWEY, G. E. BROWN JR.: Transformations of mercury, iron, and sulfur during the reductive dissolution of iron oxyhydroxide by sulfide .....	877			
J. L. MORFORD, W. R. MARTIN, L. H. KALNEJAH, R. FRANCOIS, M. BOTHNER, L.-M. KARLE: Insights on geochemical cycling of U, Re and Mo from seasonal sampling in Boston Harbor, Massachusetts, USA .....	895			
J. THERIAULT, L. CHAUVAUD, J. CLAVIER, J. GUARINI, R. B. DUNBAR, R. FICHEZ, D. A. MUCCIAKONE, E. MORIZE: Reconstruction of seasonal temperature variability in the tropical Pacific Ocean from the shell of the scallop, <i>Compsopallium vulgata</i> .....	918			
K. A. MERRITT, A. AMIRBAIDMAN: Mercury dynamics in sulfide-rich sediments: Geochemical influence on contaminant mobilization within the Penobscot River estuary, Maine, USA .....	929			
M. E. KYLANDER, J. MULLER, R. A. J. WÖST, K. GALGATHER, R. GARCIA-SANCHEZ, B. J. COLES, D. J. WEISS: Rare earth element and Pb isotope variations in a 52 kyr peat core from Lynch's Crater (NE Queensland, Australia): Proxy development and application to paleoclimate in the Southern Hemisphere .....	942			
<i>Continued on outside back cover</i>				

This article was originally published in a journal published by Elsevier, and the attached copy is provided by Elsevier for the author's benefit and for the benefit of the author's institution, for non-commercial research and educational use including without limitation use in instruction at your institution, sending it to specific colleagues that you know, and providing a copy to your institution's administrator.

All other uses, reproduction and distribution, including without limitation commercial reprints, selling or licensing copies or access, or posting on open internet sites, your personal or institution's website or repository, are prohibited. For exceptions, permission may be sought for such use through Elsevier's permissions site at:

<http://www.elsevier.com/locate/permissionusematerial>



## Effects of *in situ* biostimulation on iron mineral speciation in a sub-surface soil

Joseph W. Stucki<sup>a,\*</sup>, Kangwon Lee<sup>a</sup>, Bernard A. Goodman<sup>a</sup>, Joel E. Kostka<sup>b</sup>

<sup>a</sup> University of Illinois at Urbana-Champaign, Department of Natural Resources and Environmental Sciences, Urbana, IL 61801, USA

<sup>b</sup> Florida State University, Department of Oceanography, Tallahassee, FL 32306, USA

Received 24 May 2006; accepted in revised form 2 November 2006

### Abstract

The *in situ* alteration of Fe redox states in subsurface soils by bacteria, otherwise known as bioreduction, may play a key role in the immobilization of hazardous redox active metals such as U, Tc, and Cr. The objective of this study was to characterize changes in Fe mineralogy occurring in a subsurface soil as a result of biostimulation in order to evaluate the bioremediation potential of this approach. Biostimulation was achieved by injecting glucose into the soil through a small well next to a sampling well. Cores taken from the sampling well were analyzed by variable-temperature <sup>57</sup>Fe Mössbauer spectroscopy. Results revealed that biostimulation resulted in an overall loss of Fe from the system and major changes in the distribution of its oxide and oxyhydroxide mineral forms. Compared to the non-biostimulated soil, the spectral components assigned to goethite were greatly diminished in intensity in the samples that had been biostimulated, whereas the hematite component was appreciably increased. The Fe(II):Fe(III) ratio in the non-oxide phase (aluminosilicate clay minerals) also increased, indicating that the bioreduction processes in the soil also affected the redox state of Fe in the constituent clay minerals.

© 2006 Elsevier Inc. All rights reserved.

### 1. Introduction

Intense efforts are underway to remediate radionuclide contaminated soils by stimulating the growth of indigenous bacteria to promote the *in situ* immobilization of U, Tc, Cr, and other harmful metals generated from nuclear power and weapons production (Kukkadapu et al., 2001; Senko et al., 2002, 2005; Petrie et al., 2003; Fredrickson et al., 2004; Istok et al., 2004; North et al., 2004; Michalsen et al., 2006). To stimulate bacterial activity in the sub-surface soils, a carbon source such as ethanol, acetate, or glucose can be injected into the soil through a small-diameter well. The reducing environment created by bacterial activity affects all redox-sensitive constituents in the soil, including the ubiquitous Fe-bearing minerals, and impacts synergistic relationships among these minerals

and the target radionuclides in the system. Iron is by far the most abundant redox-active metal in the soil and cycling between Fe(II) and Fe(III) is a prominent factor affecting chemical processes in soils, especially where large periodic changes in water contents occur (Ponnamperuma, 1972). The oxidation state of Fe thus provides a valuable indicator of the redox status of the soil and greatly influences redox processes.

Among the Fe-bearing minerals in soils, the most common are aluminosilicate clay minerals and iron oxides or oxyhydroxides (Schwertmann, 1988). The oxidation state of structural Fe in the clay minerals alters the physical-chemical properties of their surfaces (Stucki, 2006) and reducing environments greatly enhance the dissolution potential of the Fe oxides, which generally control the levels of Fe in solution. The particular Fe oxide mineral phase also influences the chemical behavior of other elements in the system. For example, Dodge et al. (2002) reported that when U is co-precipitated with maghemite, magnetite, or goethite, the uranium species are oxyhydroxides and are

\* Corresponding author. Fax: +1 217 244 7805.  
E-mail address: [jstucki@uiuc.edu](mailto:jstucki@uiuc.edu) (J.W. Stucki).

readily dissolved in concentrated HCl, whereas with lepidocrocite and ferrihydrite the uranium species resist dissolution. If U is co-precipitated with green rust, it is in the U(IV) form. Upon exposure to air, both U and green rust are oxidized rapidly, which converts green rust to magnetite and remobilizes the U. Understanding how the Fe minerals are affected by biostimulation in soils thus can give key insight into the behavior of targeted redox-active species. It also aids in the development of reliable theoretical models as valuable tools for predicting the fate of U in contaminated soils. At present, the utility of such models is marginalized because of the lack of reliable information about the behavior of Fe minerals in the system.

The purpose of the current study was to narrow that gap by characterizing changes in Fe mineralogy occurring in a biostimulated soil using variable-temperature Mössbauer spectroscopy. The objective was to investigate how Fe minerals are affected by biostimulation in the U-contaminated soils. This is by no means a straightforward exercise, since several Fe-containing phases could be present and a considerable fraction of the Fe could be of a poorly crystalline or amorphous nature. The overall Fe concentrations are, moreover, only about 5–6 mass % of the soil. These mineral forms are, therefore, difficult to identify by conventional X-ray powder diffraction.

## 2. Materials and methods

The samples used were obtained from contaminated and biostimulated subsoils at the US Department of Energy (DOE) Field Research Center (FRC) at Oak Ridge National Laboratory, Tennessee. These soils were contaminated with varying amounts of U and Tc, among other elements, over a period of more than two decades and have been investigated through a series of single-well, push-pull tests to determine the feasibility of using in situ biostimulation as a means for radionuclide immobilization. Studies (Petrie et al., 2003; Istok et al., 2004; North et al., 2004) found that indigenous Fe-reducing bacteria responded to injection of electron donors (acetate, glucose, or ethanol) by catalyzing the reduction and immobilization of U(VI) in the soil. The mineralogy and redox state of Fe in the surrounding soil minerals are believed to play an important role in this process. In order to characterize these changes in the Fe minerals more completely, parallel samples to those investigated by Petrie et al. (2003) and North et al. (2004) were submitted to analysis by variable-temperature Mössbauer spectroscopy. The samples selected were: (1) FWB302 taken from an uncontaminated background area; (2) FWB032-01-05 taken from the contaminated subsoil (without biostimulation) in push-pull well identified by Istok et al. (2004) as FW32; and (3) FB45-01-42 taken from the glucose biostimulated subsoil in a nearby well labelled FB45 by Istok et al. (2004). The reader should consult Petrie et al. (2003) and North et al. (2004) for

further information about these samples. A limited number of analyses were also performed on cores removed from wells labelled FW27, FW31, FW33, and FW34, which were located near well FW32.

After sampling, care was taken to protect the samples from the atmosphere and from significant bacterial activity by enclosing them in Ar purged tubes at the site, then freezing them to 77 K in liquid nitrogen (see description by North et al., 2004). Samples were kept frozen until used, then inert atmosphere techniques were used in order to minimise changes in oxidation state during laboratory handling (Stucki et al., 1984). No attempt was made to dry or homogenize samples by grinding or extensive mixing; sub-samples were selected for study by manually removing large (predominantly quartz) grains by eye under a N<sub>2</sub> atmosphere. Samples were analyzed for Fe(II) and total Fe using the 1,10-phenanthroline method of Komadel and Stucki (1988), which, unlike the commonly used Ferrozine method (Stookey, 1970; Lovley and Phillips, 1986), is reliable for the quantitative determination of the different oxidation states of Fe in both silicate and oxide minerals.

### 2.1. Mössbauer spectroscopy

Mössbauer spectra were acquired in transmission mode using a Web Research (Edina, Minnesota) spectrophotometer equipped with a Janis (Wilmington, Massachusetts) Model SHI-850-5 closed cycle refrigerator (CCR) cryostat. This cryostat is capable of reaching

Table 1  
Temperatures at which magnetic hyperfine interactions are observed for Fe oxides and oxyhydroxides as sextet lines in the Mössbauer absorption spectrum (from Stevens et al., 1983; Murad and Johnston, 1987; Murad, 1988)

Iron oxide/ oxyhydroxide	Magnetic ordering temperature (K)	Hyperfine magnetic field, $B_{\text{hf}}$ (T)	Temperature (K) of Mössbauer spectrum
Hematite	955	51.8 at 295	298
		53.5 <sup>a</sup> , 54.2	77
		53.3 <sup>a</sup> , 54.2	4.2
Magnetite Maghemite	850 743–985	49.2, 46.3, and 45.1	298
		50.0	298
		52.6	77
		52.6	4.2
Goethite (well crystallized)	393	38.2	298
Goethite (poorly crystallized)	<77	50.0	77
		50.6	4.2
Lepidocrocite	<77	45.8, 52.5	4.2
Ferrihydrite (6-line)	<77	49.3, 50.0	4.2
Ferrihydrite (2-line)	<77	46.5	4.2

<sup>a</sup> Above the Morin transition temperature.

sample temperatures in the region of 4.2 K without the addition of cryogenic liquids. The sample temperature was controlled with a Web model WTC-102 autotuning temperature controller. Spectra were acquired into 1024 channels with a drive system operating with a triangular waveform using a  $^{57}\text{Co}$  in Rh source of nominal strength 50 mCi (1.85 GBq) (Ritverc GmbH, St Petersburg, Russia).

A 7- $\mu\text{m}$  natural abundance Fe foil was used for velocity calibration of the spectrophotometer and isomer shifts are expressed relative to the center of the iron metal resonance. Spectra at the various temperatures were initially interpreted according to the guidelines listed in Table 1, which reports generalizations from the literature regarding the mineral(s) that will likely be observed at the various sample temperatures.

## 2.2. Data analysis

Analyses of the Mössbauer spectra were performed assuming Lorentzian line shapes. Specific site analysis was carried out by initializing the iterative fitting procedure with estimated values for the isomer shift ( $\delta$ ), quadrupole splitting ( $\Delta$ , doublet lines), quadrupole shift ( $\epsilon$ , sextet lines), line width, component area, and magnetic hyperfine field ( $B_{\text{hf}}$ , sextet lines), then allowing the program to optimize the fit to converge to a  $\chi^2$  value as close to 1.00 as possible. Hyperfine parameters for the doublet components obtained from the site-analysis method were then used as fixed values in the method

for calculating the hyperfine field distributions (HFD). The HFD of the sextet component was determined by fixing  $\delta$ ,  $\epsilon$ , and line width and calculating the probability (intensity  $\times$  line width of the transition) for many incremental values of  $B_{\text{hf}}$  over the expected range for Fe oxides and oxyhydroxides. To further optimize the fitting procedure and to achieve internal consistency, the maximum probability values for  $B_{\text{hf}}$  were then entered back into the site analysis routine to yield the results reported in Table 2. Spectra illustrated in Figs. 2 and 3 resulted from the site analysis method and the HFD are presented in Fig. 4.

## 3. Results and interpretation

Mössbauer spectra (Figs. 1–3) from samples at 298, 77, and 4.2 K all consisted of a mixture of sextet and doublet components arising from Fe(III) in iron oxides and oxyhydroxides (hereafter referred to as Fe oxides) and from Fe(III) and Fe(II) in aluminosilicate clay minerals. The spectral component assigned to Fe(III) in aluminosilicate clay minerals could also partly correspond to low spin Fe(II) from minerals such as pyrite. However, since this mineral phase would not be expected to decrease under the conditions of the present experiment, its possible presence would have no effect on any of the conclusions from the present study. Hyperfine field distributions (HFD) demonstrated the existence of multiple sextets of magnetically ordered components in the samples at each temperature (Fig. 4).

Table 2  
Mössbauer hyperfine parameters from radionuclide contaminated sub-surface soil before and after biostimulation with glucose

Soil treatment	$T$ (K)	Peaks	Fe Ox. state	Hyperfine parameters						
				$\delta$ (mm/s)	$\Delta$ or $\epsilon$ (mm/s)	$B_{\text{hf}}$ (T)	Area (%)	$\chi^2$		
Non-biostimulated	298	Doublet 1	Fe(III)	0.27	0.58	n/a	81.9	0.98		
		Doublet 2	Fe(II)	1.05	2.82	n/a	9.2			
		Sextet 1	Fe(III)	0.43	-0.10	51.1	8.9			
	77	Doublet 1	Fe(III)	0.36	0.70	n/a	37.0	1.39		
		Doublet 2	Fe(II)	1.14	3.14	n/a	7.9			
		Sextet 1	Fe(III)	0.52	-0.99	47.5	52.4			
		Sextet 2	Fe(III)	0.54	-0.01	53.3	2.7			
		4.2	Doublet 1	Fe(III)	0.37	0.73	n/a		32.5	1.72
			Doublet 2	Fe(II)	1.15	3.12	n/a		5.7	
	Biostimulated with glucose	298	Doublet 1	Fe(III)	0.29	0.64	n/a	68.2	1.38	
			Doublet 2	Fe(II)	1.08	2.84	n/a	16.6		
			Sextet 1	Fe(III)	0.47	-0.08	51.7	15.2		
77		Doublet 1	Fe(III)	0.37	0.69	n/a	51.1	1.19		
		Doublet 2	Fe(II)	1.17	3.02	n/a	17.5			
		Sextet 1	Fe(III)	0.54	-0.09	46.7	17.2			
		Sextet 2	Fe(III)	0.55	-0.03	53.2	14.1			
		4.2	Doublet 1	Fe(III)	0.38	0.74	n/a		48.2	1.31
			Doublet 2	Fe(II)	1.18	3.11	n/a		12.6	
4.2		Sextet 1	Fe(III)	0.52	-0.66	49.6	18.4	1.31		
		Sextet 2	Fe(III)	0.44	-0.01	53.4	17.2			
		Sextet 3	Fe(III)	0.52	-0.05	46.5	3.6			

n/a, not applicable.

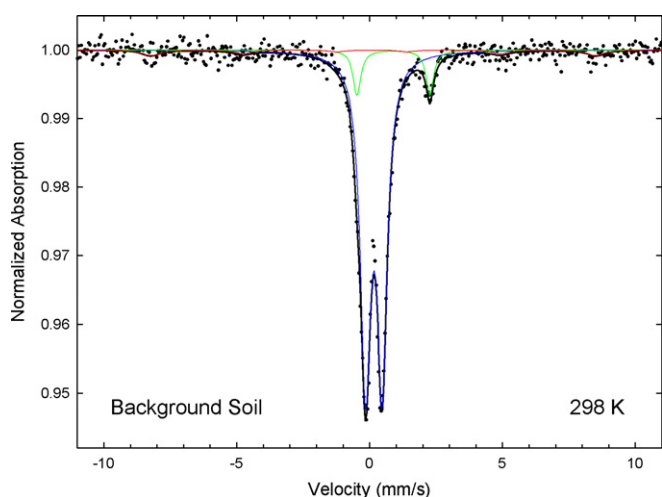


Fig. 1. Mössbauer spectrum of FRC background sub-surface soil from well FW302, without biostimulation, at 298 K, including components from curve fitting using a site analysis algorithm. Relative peak areas: Fe(III) doublet, 85.8%; Fe(II) doublet, 9.2%; Fe(III) sextet, 4.9%.

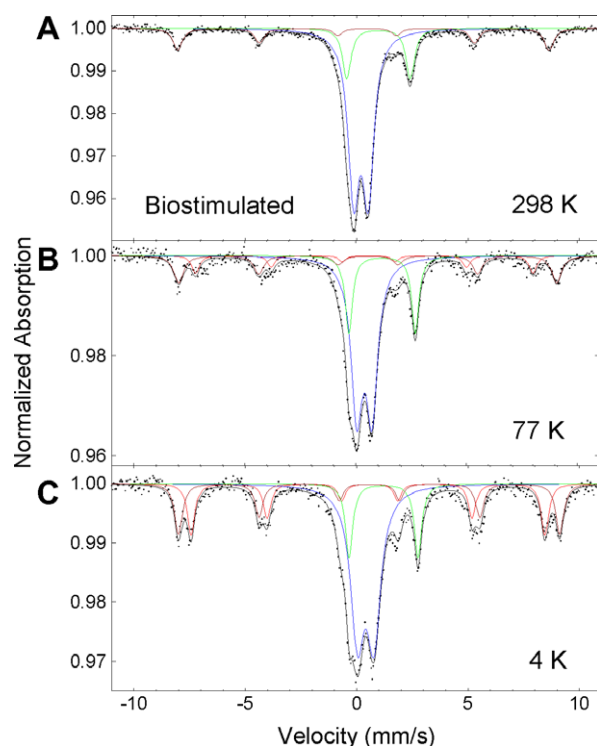


Fig. 3. Mössbauer spectra of FRC contaminated sub-surface soil from well FW032, after biostimulation with glucose, at 298 K (A), 77 K (B), and 4.2 K (C), including components from curve fitting using a site analysis algorithm. Hyperfine parameters are given in Table 2.

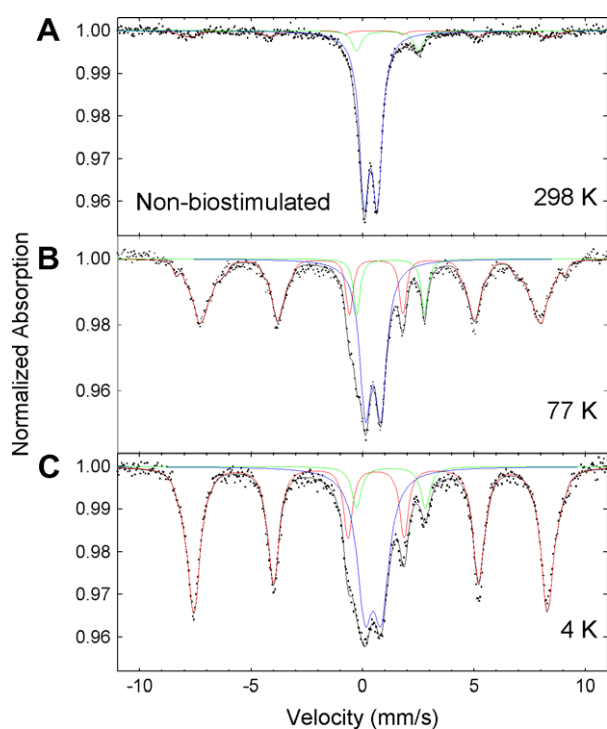


Fig. 2. Mössbauer spectra of FRC contaminated sub-surface soil from well FW032, without biostimulation, at 298 K (A), 77 K (B), and 4.2 K (C), including components from curve fitting using a site analysis algorithm. Hyperfine parameters are given in Table 2.

The Mössbauer spectrum at room temperature (Fig. 1) of the background soil material (FW302) revealed relative peak areas for hematite to be about 4.6% and of Fe(II) in the phyllosilicate phase to be about 9.2%, with the remaining area attributable to Fe(III) in the phyllosilicate and non-magnetically ordered Fe oxide phases such as goethite. Spectra (not shown) from wells FW27, FW31, FW33, and

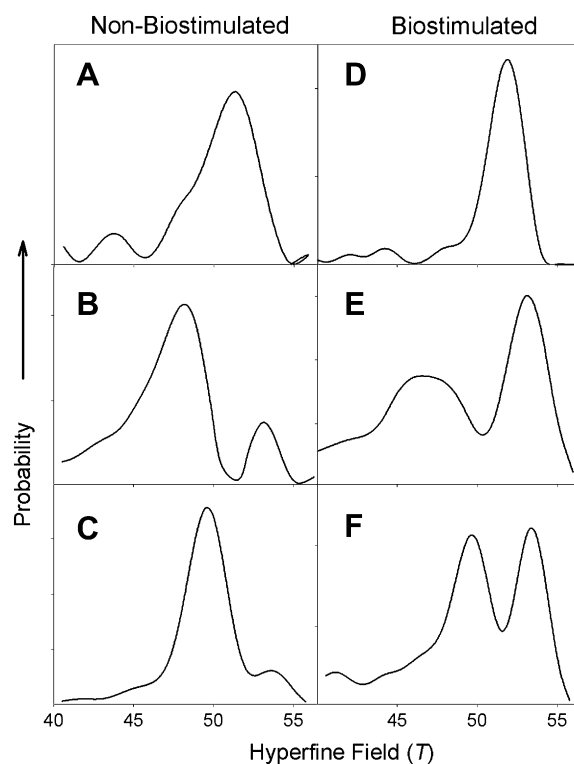


Fig. 4. Hyperfine field distributions (HFD) from Mössbauer spectra of FRC contaminated sub-surface soil from well FW032, before (A–C) and after (D–F) biostimulation with glucose, at 298 K (A and D), 77 K (B and E), and 4.2 K (C and F).

Table 3  
Total Fe and Fe(II) contents of contaminated soil before and after biostimulation

Treatment	Fe(II)		Total Fe <sup>a</sup>	
	mmol/g sample	% of total Fe	mmol/g sample	wt% of sample
No biostimulation	0.070	6.87	1.024	5.72
Biostimulated with glucose	0.093	11.07	0.841	4.70

<sup>a</sup> Includes both Fe oxide and aluminosilicate clay mineral phases.

FW34 revealed similar low amounts of hematite in their Mössbauer spectra. A relatively low hematite content thus appears to be the general trend throughout the soils of the study area and others (Kukkadapu et al., 2006; Michalsen et al., 2006) reported similar results.

Chemical analysis of the contaminated soil (Table 3) showed that biostimulation decreased the total Fe content of the sample from 1.024 mmol Fe/g sample (5.7 wt%) to 0.84 mmol Fe/g sample (4.7 wt%) and increased the Fe(II) content from 0.07 mmol Fe/g sample (6.87% of total Fe) to 0.093 mmol Fe/g sample (11.07% of total Fe). Results from the 4.2 K Mössbauer spectra showed similar values with the Fe(II) component increasing from 5.7% to 12.6% of the spectral area (Table 2).

The fraction of Fe giving sextets increased progressively with decreasing temperature in all cases. *In situ* biostimulation clearly invoked further significant alterations in the spectra, indicating transformations in the Fe oxides and changes in oxidation state of the structural Fe in the aluminosilicate clay mineral. These results will now be described in more detail according to the recording temperature.

### 3.1. 298 K

The Mössbauer spectrum of the non-biostimulated sub-soil at 298 K (Fig. 2A) was dominated by a Fe(III) doublet, with secondary peaks due to Fe(II) and a magnetically ordered Fe(III) component (Fig. 4A). The Fe(II) is assigned to structural sites in aluminosilicate phases. The magnitude of its quadrupole splitting allows elimination of the presence of significant amounts of solvated Fe<sup>2+</sup> in cation exchange sites. The sextet component arises from Fe(III) in magnetically ordered Fe oxide phases and the Fe(III) doublet represents both Fe(III) in the aluminosilicate phase and in Fe oxide phases that are not magnetically ordered at that temperature.

The existence of a sextet at room temperature is normally indicative of the presence of hematite, magnetite, and/or maghemite (Table 1). The magnetic hyperfine field distribution (HFD) (Fig. 4A) revealed the most probable  $B_{\text{hf}}$  value to be 51.4 T and the quadrupole shift was  $-0.28$  mm/s (Table 2). Passing a magnet through the sample failed to scavenge any mineral particles, so maghemite and magnetite were considered unlikely, although small amounts could have been present but evaded detection by this

method. Hematite would appear, therefore, to be the Fe oxide that is responsible for this magnetic hyperfine structure. The rather broad distribution in magnetic field values (Fig. 4A) further suggests that the hematite has variable levels of crystallinity and/or Al substitution.

Biostimulation caused an overall decrease in the total Fe content of the sample (Table 3), but increased the Mössbauer spectral intensity of the sextet component relative to the doublets at 298 K (Table 2; compare Figs. 2A and 3A). Biostimulation, therefore, preferentially dissolved the Fe phase that was non-magnetically ordered at this temperature and/or converted some of the non-magnetically ordered Fe phase into a magnetically ordered phase. The HFD (Fig. 4D) revealed, in fact, that the magnetically ordered phase is better organized than prior to biostimulation, with a single dominant probability at  $B_{\text{hf}} = 52.0$  T, corresponding to a reasonably well defined hematite (Table 2). Biostimulation, therefore, apparently increased the amount of hematite and possibly improved its crystallinity.

The intensity of the Fe(II) doublet (its higher velocity component clearly resolved at about 2.6 mm/s) also increased from about 9.2% to 16.6% of the total absorption intensity as structural Fe in the aluminosilicate clay mineral became more reduced by bacterial activity. Biostimulation thus altered both the Fe oxide and aluminosilicate phases.

Notice, further, that the relative intensity of the Fe(II) doublet varies with temperature (Table 2). Such variations may arise from differences in the recoil-free fractions of absorbed  $\gamma$  rays by the various Fe(II) and Fe(III) components. Spectra at the lowest possible temperature are normally preferred in making this calculation because any differences in recoil-free fraction will be at a minimum. The recoil-free fraction for Fe(II) is normally lower than that for Fe(III) in similar structures, which should cause the relative area of Fe(II) to Fe(III) to increase with decreasing temperature. Interestingly, the opposite was found in the current study. The reason is probably the consequence of the recoil-free fraction of poorly crystalline Fe oxides (which contain much of the Fe(III) in these samples) being lower than that of the aluminosilicate minerals (which contain the Fe(II)).

### 3.2. 77 K

Cooling the non-biostimulated sample to 77 K generated considerable sextet structure with two distinct components, which were clearly visible in both the absorption spectrum (Fig. 2B) and the HFD (Fig. 4B). The dominant sextet was at  $B_{\text{hf}} = 48.4$  T and is assigned to goethite because this hyperfine field, as well as the other hyperfine parameters (Table 2), are within the range reported for Al-substituted goethites (e.g., Golden et al., 1979; Goodman and Lewis, 1981; Murad and Schwertmann, 1983). The weaker sextet in Fig. 2B was at  $B_{\text{hf}} = 53.1$  T and is

assigned to hematite in accordance with the room-temperature spectra.

In the biostimulated sample, the intensity of the goethite phase was much lower than in the non-biostimulated sample, and at the same time the level of the hematite phase increased (compare Figs. 2B and 3B). This increase was greater than seen in the results at 298 K, indicating that not all of the hematite showed magnetic hyperfine structure at room temperature, and that this phase contains a range of particle sizes and/or different levels of Al substitution. The HFD of the biostimulated sample (Fig. 4E), like the non-biostimulated sample, also contained two general maxima. Unlike the non-biostimulated sample, however, the hematite phase with  $B_{\text{hf}} = 53.1$  T was more dominant in the biostimulated sample (Table 2).

Biostimulation increased the Fe(II) doublet at 77 K from 7.9% to 17.5%. (Table 2) These values differ slightly from those observed at 298 K, but are within the errors expected for statistical uncertainties in the curve fitting.

### 3.3. 4.2 K

At 4.2 K the sextet pattern in the non-biostimulated soil was dominated by one goethitic component (Figs. 2C and 4C). The hematite, though still visible, was only a minor feature. At this temperature, all of the Fe oxides should be magnetically ordered, so Figs. 2C and 4C provide a clear view of the distribution of Fe among the various possible phases, revealing that the Fe oxides accounted for about 60% of the Fe in the non-biostimulated sample and goethite comprised over 90% of the Fe oxide (Table 2). The hematite phase accounted for about 6% of the total Fe and the aluminosilicate phase for about 38%. About 18% of the Fe in the aluminosilicate was in the Fe(II) state. The HFD for the non-biostimulated sample shows little probability in the range 45–47 T, indicating little if any ferrihydrite in this sample.

A comparison of the relative intensities of the goethite component at the different temperatures also gives an impressive example of how the magnetic order of this mineral increases with lower temperatures. At 298 K, the goethite spectrum is collapsed under the central doublet and thus is indistinguishable from other non-magnetically ordered Fe phases, including Fe(III) in the aluminosilicate clay minerals. At 77 K, peaks could be assigned positively to the goethite phase, but its total abundance was unclear because of the possible presence of a disordered Al-rich fraction that remained as a doublet in the Mössbauer spectrum at that temperature. At 4.2 K, however, all of the Fe oxide components show magnetic hyperfine structure and the goethite phase is clearly evident (Figs. 2C and 4C). Studies of soils and subsoils by Mössbauer spectroscopy which exclude measurements at or near 4.2 K (e.g., Zachara et al., 2004; Kukkadapu et al., 2005) are, therefore, limited in their ability to diagnose correctly the Fe oxides in the system.

Comparing the spectra at 4.2 K for the non-biostimulated soils (Figs. 2C and 4C) with those that had been biostimulated (Figs. 3C and 4F) revealed that biostimulation caused dramatic changes in the Fe mineralogy of this sub-surface soil. The first important difference was that the sextet pattern at 4.2 K was much less intense than in the non-biostimulated sample (from about 56% of the total area to about 39%; Table 2; compare Figs. 2C and 3C). These values are in excellent agreement with the analytical data (Table 3) which showed that about 18% of the total Fe was lost as a result of biostimulation. Apparently the phase lost was almost entirely goethite.

Second, a prominent splitting was introduced into the outermost peaks of the sextet (Figs. 3C and 4F), which resolved into two distinct HFD components; with  $B_{\text{hf}} = 49.6$  and 53.4 T, and into a third, less obvious sextet with  $B_{\text{hf}} = 46.5$  T. Before biostimulation the goethite peak dominated the HFD at 4.2 K, with a minor contribution from hematite (Fig. 2C and 4C). The magnetic hyperfine field for goethite at 4.2 K is 50 T; which compares well with the observed value of 49.6 T. The  $B_{\text{hf}}$  value for hematite in the biostimulated sample is 53.4 T, but the quadrupole shift ( $\epsilon$ ) is still negative, revealing that the hematite phase failed to undergo the Morin transition.

Third, the small sextet with  $B_{\text{hf}} = 46.5$  T could be ferrihydrite (Murad and Schwertmann, 1980). Note that, in contrast to the other common Fe oxide minerals, ferrihydrite has a highly disordered structure, which is related to that of hematite but with some vacant Fe sites and some of the O replaced by  $\text{H}_2\text{O}$ . This mineral exhibits no magnetic hyperfine structure at 77 K, but, if present, at 4.2 K

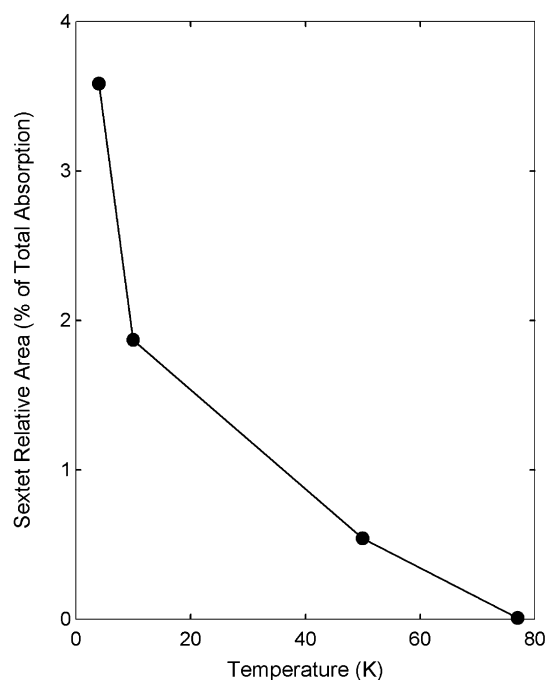


Fig. 5. Effect of temperature on relative area of sextet component tentatively assigned to ferrihydrite in biostimulated sub-surface soil.

it will have parameters similar to those given in Table 2 for sextet 3. The relative area of this sextet also increases with decreasing temperature from 77 to 4.2 K (Fig. 5), thus providing further evidence that this feature could indeed be due to ferrihydrite.

And fourth, the efficacy of bacteria as *in situ* reducers of Fe in soil aluminosilicate clay minerals was made clear by the increase in Fe(II) content from 5.8% of total Fe to 12.6% after bioreduction. This extent of reduction of structural Fe is sufficient to yield large differences in the surface chemistry of the constituent clay minerals. Among the possible impacts of this change in the redox status of the aluminosilicate clay minerals are an increase in cation exchange capacity, decrease in specific surface area, increase in cation fixation capacity, decrease in swelling, increased potential for nitrate reduction, increase in surface pH, and enhanced degradation of organics (Stucki, 2006; Stucki and Kostka, 2006).

#### 4. Discussion

Biostimulation with glucose resulted in a loss of Fe from the soil, as evidenced by the total Fe contents. This decrease could be accounted for entirely by an overall decrease in the Fe oxide components. The aluminosilicate structures, on the other hand, seemed to remain intact and their Fe(II):Fe(III) ratio increased, indicating that these clay minerals were involved in the redox processes associated with biostimulation. The loss of Fe also involved major changes in the relative levels of the various Fe oxide mineral forms. Biostimulation caused a large decrease in the level of the goethite component, accompanied by an appreciable increase in the amount of hematite and the possible generation of a small residual quantity of ferrihydrite.

An interesting comparison can be made between the present results from *in situ* biostimulation and those reported by Kukkadapu et al. (2006) from a laboratory-based *ex situ* study of the biotransformation of Fe in a soil sample from the same site as that used in the present investigation. Kukkadapu et al. (2006) reported that goethite and phyllosilicate were the major Fe-containing phases and that Fe(III) in both mineral types was partially reduced by the bacteria. Goethite reduction, however, was enhanced in the presence of the electron shuttle anthraquinone-2,6-disulfonate (AQDS). To this extent their results bear a close relationship to the present ones. In contrast to the present experiments, however, Kukkadapu et al. (2006) observed no dissolution of Fe and found no transformation product from goethite, although they speculated the presence of a surface-associated phase on the residual goethite. They detected no formation of hematite, although a minor hematite component (accounting for ~5% of the Fe) was present in their samples.

One question that arises concerning the present experiments is the extent to which the observed results might be the result of a natural variation in the Fe mineral speciation rather than showing the effect of biostimulation. In-

deed, considerable local variations in hematite:goethite ratios in soils have been reported over distances of a few centimeters (e.g. Childs et al., 1978). However, as noted above, specimens from non-biostimulated cores from the Oak Ridge site have been studied using Mössbauer spectroscopy both by ourselves and others (e.g. Kukkadapu et al., 2006; Michalsen et al., 2006), and in every case the hematite level was either low or undetectable. The high level of hematite in our present biostimulated specimen is thus unlikely to be the result of simply a natural variation in composition of the original soil, although this possibility cannot be completely excluded.

Further corroboration that the changes in properties between the unbiostimulated and the biostimulated samples were induced by microbial activity is found in a study by North et al. (2004), who conducted a parallel investigation of samples from the same sediment cores as the present study. Using wet chemical extractions, they observed a doubling of the reduced Fe content, similar to that reported here in Tables 2 and 3. They found further that microbial communities also showed large differences before and after biostimulation that could be attributed directly to the change in Fe oxidation state (North et al., 2004), namely, a quantitative increase in genetic sequences of Fe-reducing bacteria was observed in parallel soil samples. The geochemical differences observed between soil samples were also supported by visual observations: unstimulated samples always had the same reddish brown color, whereas the biostimulated samples were darker brown to green.

The changes in Fe mineralogy observed in the current experiments are contrary to those that generally occur in soils, where the conversion of hematite to goethite, rather than vice versa, is a common phenomenon (Schwertmann, 1971, 1984). What then are the reasons for the present results?

Some insight into the processes involved can be obtained by considering the mechanisms by which hematite, goethite, and ferrihydrite are formed in soils. This was discussed in detail by Schwertmann (1988) who demonstrated that the form of Fe that is precipitated from soil solution is controlled by the concentration of the inorganic forms of Fe in solution. If the solubility product of ferrihydrite ( $\cong 10^{-38}$ ) is exceeded, this is the form that is precipitated; otherwise, goethite (solubility product  $\cong 10^{-42}$ ) is the mineral formed. In contrast, hematite is formed via an internal rearrangement and dehydration within ferrihydrite aggregates rather than by precipitation from solution. Hematite thus can only form if ferrihydrite is precipitated first (Murad and Schwertmann, 1986).

Both Al and organic matter in solution influence the nature of the Fe oxide that is precipitated. Complexation with organic matter decreases the activity of inorganic Fe; the solubility product of ferrihydrite is prevented from being exceeded, and goethite is formed. To illustrate this, Schwertmann (1988) described root channels in reddish palaeosols as often showing a radial zonation of Fe distribution and speciation, in which a bleached (Fe deficient)

zone immediately around the root is followed by a goethitic zone, which is free of hematite, before reaching the unaffected hematitic soil. Similarly, in soils formed in temperate climates from hematite-containing parent materials, the hematite disappears and is replaced by goethite, lepidocrocite, and/or ferrihydrite (Campbell and Schwertmann, 1984). In contrast to organic matter, the presence of Al in solution suppressed the formation of goethite *in vitro*, although Al-substituted goethites commonly occur in soils.

The results from the current experiment can, therefore, be understood only in terms of an initial dissolution of a large fraction of the original goethite as a result of biostimulation. This was then followed by reprecipitation of predominantly ferrihydrite, which was subsequently transformed to hematite. Incomplete reprecipitation explains the net loss of Fe oxide from the system. The presence of only a small amount of ferrihydrite in the biostimulated soil suggests that the rate of ferrihydrite transformation to hematite was faster than the rate of ferrihydrite reprecipitation and/or the transformation step from ferrihydrite to hematite was almost complete at the time of sampling. Generally ferrihydrite and hematite are not found together in soils, because the rate of formation of ferrihydrite, which is determined by the rate of Fe release from (primarily) silicate minerals, is slower than the rate of transformation of ferrihydrite to hematite (Schwertmann, 1988). This appears also to be the case in the biostimulated soils.

The soil may, however, still be in a state of transition and further changes in the Fe speciation might be expected in future years. For example, Fey (1983) reported that in soils containing both hematite and goethite, hematite is reduced faster than goethite. The creation of a reducing environment might be expected to lead to preferential reduction of hematite to Fe(II), thereby increasing the fraction of Fe as goethite, which may also form by Fe(II) reoxidation if the conditions are appropriate. With increasing time the present soils might, therefore, be expected to show a decrease in the hematite level as a result of subsequent dissolution and recycling. With increasing levels of organic matter from bacterial residues, some regeneration of goethite may also occur.

In order to understand systems such as the one in the present experiments, sampling over periods of many years is imperative so that the consequences of changes in microbial activity on the mineralogical forms of Fe oxides can be fully evaluated. Since the Fe mineralogy has a major effect on the chemistry of the pollutant elements whose control is the reason for these experiments, the availability of such information to scientists developing models for predicting the long-term chemistry of pollutant molecules, such as U in sub-surface soils, is essential.

Kukkadapu et al. (2005) recently reported the bioreduction of a mixture of ferrihydrite and akaganéite ( $\beta$ -FeO-OH) by *Shewanella putrefaciens* under anoxic conditions with lactate as electron donor and anthraquinone-2,6-disulfonate as an electron shuttle. They found that reduc-

tion was rapid, 60% of the Fe being reduced within one day and only a further 10% over the following three years. They reported that magnetite was the initial product in their experiments, but it was unstable and was subsequently transformed into ferrous hydroxyl carbonate. The striking difference between those results and the ones from the present study indicate that the mechanisms of bioreduction of Fe oxide minerals in soils is extremely complex and requires considerable additional effort in order to achieve even a basic understanding of the processes involved.

## 5. Conclusions

Biostimulation has a marked effect on the Fe mineralogy of subsurface soil. Once dominated by goethite, the subsoil after biostimulation contained about equal amounts of goethite and hematite, but the total Fe oxide content was only about two-thirds as much as before. Biostimulation also resulted in an increase in the fraction of the Fe in the high spin Fe(II) form, which is presumably in aluminosilicate minerals. This increase was greater than that which results from a decrease in the overall Fe content of the soil as a result of the removal of oxide components and indicates that reduction of Fe(III) to Fe(II) in the aluminosilicate clay mineral framework was also induced by biostimulation. The ratio of doublets at 4.2 K attributable to Fe(II) and Fe(III) in the aluminosilicate increased, respectively, from 0.18 in the non-biostimulated sample to 0.26 in the biostimulated sample.

The transformation of goethite to ferrihydrite then hematite as a result of biostimulation may be highly significant in the context of understanding the long term effects on the chemistry of U at these sites. If U precipitation occurs simultaneously with hematite formation, then the nature of the chemical association between these components will, to a large extent, determine the geochemical stability of the reduced U species. Obtaining this information should be a fundamental research priority.

The importance of variable-temperature (4.2–298 K) Mössbauer spectroscopy in this work cannot be over emphasized. This is the only technique able to give good information on the Fe speciation in these complex mineralogical specimens in their natural forms. The ability to examine this entire temperature range is critical because components such as ferrihydrite can only be detected with confidence at the lowest temperature. Because these analyses were conducted on relatively small sub-samples (a few hundred milligrams), much larger numbers of specimens need to be investigated in order to determine the likely effects that could arise from natural geological variability in samples from contaminated sites such as the DOE-FRC at Oak Ridge.

## Acknowledgments

The authors gratefully acknowledge financial support from the Environmental Remediation Science Program

(ERSP), Division of Biological and Environmental Research (BER), US Department of Energy, Grant No. DE-FG02-00ER62986 and subcontract FSU F48792; and from the National Science Foundation, Division of Petrology and Geochemistry, Grant No. EAR 01-26308. This project was also supported by a fellowship to J.E. Kostka from the Hanse Wissenschaftskolleg.

Associate editor: Carrick M. Eggleston

## References

- Campbell, A.S., Schwertmann, U., 1984. Iron oxide mineralogy of placic horizons. *J. Soil Sci.* **35**, 569–582.
- Childs, C.W., Goodman, B.A., Churchman, G.J., 1978. Application of Mössbauer spectroscopy to the study of iron oxides in some red and yellow-brown soil samples from New Zealand. *Dev. Sedimentol.* **27**, 555–565.
- Dodge, C.J., Francis, A.J., Gillow, J.B., Halada, G.P., Eng, C.W., Clayton, C.R., 2002. Association of uranium with iron oxides typically formed on corroding steel surfaces. *Environ. Sci. Technol.* **36**, 3504–3511.
- Fey, M.V., 1983. Hypothesis for the pedogenic yellowing of red soil materials. *Technical Communication, Department of Agriculture and Fisheries, Republic of South Africa* **18**, 130–136.
- Fredrickson, J.K., Zachara, J.M., Kennedy, D.W., Kukkadapu, R.K., McKinley, J.P., Heald, S.M., Liu, C., Plymale, A.E., 2004. Reduction of  $\text{TeO}_4^-$  by sediment-associated biogenic Fe(II). *Geochim. Cosmochim. Acta* **68**, 3171–3187.
- Golden, D.C., Bowen, L.H., Weed, S.B., Bigham, J.M., 1979. Mössbauer studies of synthetic and soil-occurring aluminum-substituted goethites. *Soil Sci. Soc. Am. J.* **43**, 802–808.
- Goodman, B.A., Lewis, D.G., 1981. Mössbauer spectra of aluminous goethites ( $\alpha\text{-FeOOH}$ ). *J. Soil Sci.* **32**, 351–363.
- Istok, J.D., Senko, J.M., Krumholz, L.R., Watson, D., Bogle, M.A., Peacock, A., Chang, Y.J., White, D.C., 2004. In situ bioreduction of technetium and uranium in a nitrate-contaminated aquifer. *Environ. Sci. Technol.* **38**, 468–475.
- Komadel, P., Stucki, J.W., 1988. Quantitative assay of minerals for  $\text{Fe}^{2+}$  and  $\text{Fe}^{3+}$  using 1,10-phenanthroline: III. A rapid photochemical method. *Clay Clay Miner.* **36**, 379–381.
- Kukkadapu, R.K., Zachara, J.M., Smith, S.C., Fredrickson, J.K., Liu, C., 2001. Dissimilatory bacterial reduction of Al-substituted goethite in subsurface sediments. *Geochim. Cosmochim. Acta* **65**, 2913–2924.
- Kukkadapu, R.K., Zachara, J.M., Fredrickson, J.K., Kennedy, D.W., Dohnalkova, A.C., McCready, D.E., 2005. Ferrous hydroxy carbonate is a stable transformation product of biogenic magnetite. *Am. Mineral.* **90**, 510–515.
- Kukkadapu, R.K., Zachara, J.M., Fredrickson, J.K., McKinley, J.P., Kennedy, D.W., Smith, S.C., Dong, H., 2006. Reductive biotransformation of Fe in shale-limestone saprolite containing Fe(III) oxides and Fe(II)/Fe(III) phyllosilicates. *Geochim. Cosmochim. Acta* **70**, 3662–3676.
- Lovley, D.R., Phillips, E.J.P., 1986. Availability of ferric iron for microbial reduction in bottom sediments of the freshwater tidal Potomac River. *Appl. Environ. Microbiol.* **52**, 751–757.
- Michalsen, M.M., Goodman, B.A., Kelly, S.D., Kemner, K.M., McKinley, J.P., Stucki, J.W., Istok, J.D., 2006. Bio-immobilization of U(VI) and Tc(VII) in intermediate-scale physical models of a bio-barrier. *Environ. Sci. Technol.* **40**, 7048–7053.
- Murad, E., 1988. Properties and behavior of iron oxides as determined by Mössbauer spectroscopy. In: Stucki, J.W., Goodman, B.A., Schwertmann, U. (Eds.), *Iron in Soils and Clay Minerals*. D. Reidel Publishing Company, Dordrecht, pp. 309–350.
- Murad, E., Johnston, J.H., 1987. Iron oxides and oxyhydroxides. In: Long, G.J. (Ed.), *Mössbauer Spectroscopy Applied to Inorganic Chemistry*, vol. 2. Plenum Press, New York, pp. 507–582.
- Murad, E., Schwertmann, U., 1980. The Mössbauer spectrum of ferrihydrite and its relations to those of other iron oxides. *Am. Mineral.* **65**, 1044–1049.
- Murad, E., Schwertmann, U., 1983. The influence of aluminium substitution and crystallinity on the Mössbauer spectra of goethite. *Clay Miner.* **18**, 301–312.
- Murad, E., Schwertmann, U., 1986. The influence of aluminium substitution and crystallinity on the Mössbauer spectra of hematite. *Clay Clay Miner.* **34**, 1–6.
- North, N.N., Dollhopf, S.L., Petrie, L., Istok, J.D., Balkwill, D.L., Kostka, J.E., 2004. Change in bacterial community structure during in situ biostimulation of subsurface sediment cocontaminated with uranium and nitrate. *Appl. Environ. Microbiol.* **70**, 4911–4920.
- Petrie, L., North, N.N., Dollhopf, S.L., Balkwill, D.L., Kostka, J.E., 2003. Enumeration and characterization of iron(III)-reducing microbial communities from acidic subsurface sediments contaminated with uranium(VI). *Appl. Environ. Microbiol.* **69**, 7467–7479.
- Ponnamperuma, F.N., 1972. The chemistry of submerged soils. *Adv. Agron.* **24**, 29–96.
- Schwertmann, U., 1971. Transformation of hematite to goethite in soils. *Nature* **232**, 624–625.
- Schwertmann, U., 1984. The influence of aluminium on iron oxides: IX. Dissolution of Al-Goethites in 6 M HCl. *Clay Miner.* **19**, 9–19.
- Schwertmann, U., 1988. Occurrence and formation of iron oxides in various pedoenvironments. In: Stucki, J.W., Goodman, B.A., Schwertmann, U. (Eds.), *Iron in Soils and Clay Minerals*. D. Reidel Publishing Company, Dordrecht, pp. 267–308.
- Senko, J.M., Istok, J.D., Sufita, J.M., Krumholz, L.R., 2002. In-situ evidence for uranium immobilization and remobilization. *Environ. Sci. Technol.* **36**, 1491–1496.
- Senko, J.M., Mohamed, Y., Dewers, T.A., Krumholz, L.R., 2005. Role for Fe(III) minerals in nitrate-dependent microbial U(IV) oxidation. *Environ. Sci. Technol.* **39**, 2529–2536.
- Stevens, J.G., Pollack, H., Zhe, L., Stevens, V.E., White, R.M., Gibson, J.L., 1983. *Mineral: Data*, Mössbauer Handbook Series, Mössbauer Effect Data Center, University of North Carolina, Asheville, NC, USA.
- Stookey, L.L., 1970. Ferrozine—a new spectrophotometric reagent for iron. *Anal. Chem.* **42**, 779–781.
- Stucki, J.W., 2006. Properties and behaviour of iron in clay minerals. In: Bergaya, F., Theng, B.K.G., Lagaly, G. (Eds.) *Handbook of Clay Science*, Elsevier, Amsterdam, pp. 429–482, Chapter 8.
- Stucki, J.W., Kostka, J.E., 2006. Microbial reduction of iron in smectite. *Compte Rendu Geosci.* **338**, 468–475.
- Stucki, J.W., Golden, D.C., Roth, C.B., 1984. Preparation and handling of dithionite-reduced smectite suspensions. *Clays Clay Miner.* **32**, 191–197.
- Zachara, J.M., Kukkadapu, R.K., Gassman, P.L., Dohnalkova, A., Fredrickson, J.K., Anderson, T., 2004. Biogeochemical transformation of Fe minerals in a petroleum-contaminated aquifer. *Geochim. Cosmochim. Acta* **68**, 1791–1805.